

Gravitational radiation from the oscillations of a rotating disk of dust

Gerhard Schäfer and Wilhelm Kley

Max-Planck-Gesellschaft, AG-Gravitationstheorie, Friedrich-Schiller-Universität, D-07743 Jena, Germany

(Received 19 July 1994)

A recently found analytic first-post-Newtonian-order solution to the problem of the relativistic oscillatory motion of a rotating disk of dust is applied to the determination of the gravitational-wave emission and radiation damping. The secular changes of the oscillation period and of the minimal rotation frequency at the rim of the disk are shown graphically. Gravitational waveforms are presented which take into account the damping of the disk through gravitational-wave emission. The implications for two merging white dwarfs are discussed.

PACS number(s): 04.25.Nx, 04.30.Db, 04.40.-b

I. INTRODUCTION

Gravitational-wave emission by relativistic astrophysical objects is of major interest for future gravitational-wave astronomy (see, e.g., Ref. [1]). However, solutions to Einstein's field equations under those conditions are difficult to obtain, even numerically. In addition to the inspiraling and coalescence of compact stars (white dwarfs, neutron stars) or black holes, the collapse of stars and the formation of black holes are the most important astrophysical sources of gravitational waves. Oscillating and collapsing rotating disks of dust might be a reasonable first model to study the gravitational-wave emission of possible formation processes to supernovas or black holes [2].

In a previous paper [3] (from now on paper I), the authors succeeded in finding an analytic solution for the first post-Newtonian motion of an oscillating and rotat-

ing disk of dust. In this paper, this solution will be utilized to derive the corresponding gravitational-wave emission and radiation damping. The paper treats analytically one of the simplest models which fits into the framework of post-Newtonian hydrodynamics and post-Newtonian gravitational-wave generation of continuously extended bodies [4]. A mathematically somewhat related situation, namely the gravitational-wave emission and damping of a binary system, has already been dealt with in the past [5,6].

II. GRAVITATIONAL RADIATION OF AXISYMMETRIC SOURCES

In suitable radiative coordinates the gravitational radiation field of an isolated source at rest can be represented asymptotically in the form [7]

$$h_{ij}^{\text{rad}} = \frac{G}{c^4 R} \sum_{l=2}^{\infty} \sum_{m=-l}^l \left[\left(\frac{1}{c}\right)^{l-2} {}^{(l)}I^{lm}(t - R/c) T_{ij}^{E2,lm}(\theta, \phi) + \left(\frac{1}{c}\right)^{l-1} {}^{(l)}S^{lm}(t - R/c) T_{ij}^{B2,lm}(\theta, \phi) \right], \quad (1)$$

where G , c , and R denote the Newtonian gravitational constant, the velocity of light, and the source-observer distance, respectively. The indices i and j are running over 1, 2, 3 and refer to Cartesian coordinates in asymptotic three-space. $T_{ij}^{E2,lm}$ and $T_{ij}^{B2,lm}$ are the so-called pure-spin tensor-spherical harmonics of electric [parity $(-1)^l$] and magnetic [parity $(-1)^{l+1}$] type. The harmonics are orthonormal on the unit sphere (coordinates θ and ϕ) and under complex conjugation they behave as $T^{E/B2,lm*} = (-1)^m T^{E/B2,l-m}$. The spherical radiative mass I^{lm} and current S^{lm} multipole moments depend on retarded time $(t - R/c)$. The upper prefix (l) at the moments denotes the number of time derivatives (l times). Complex conjugation results in $I^{lm*} = (-1)^m I^{l-m}$ and $S^{lm*} = (-1)^m S^{l-m}$.

In axisymmetric situations only the multipole moments with $m = 0$ can be different from zero (if the multipole decomposition has been adapted to the axis

of the body). If, additionally, the body has a maximal discrete symmetry with respect to the origin of the coordinate system, the mass moments with $l = \text{uneven}$ and the current moments with $l = \text{even}$ vanish. Thus, the radiation field of a rotating disk of dust, at the first post-Newtonian approximation, can be written in the simple form (see also [8])

$$h_{ij}^{\text{rad}} = \frac{G}{c^4 R} \left[{}^{(2)}I^{20} T_{ij}^{E2,20} + \frac{1}{c^2} {}^{(3)}S^{30} T_{ij}^{B2,30} + \frac{1}{c^2} {}^{(4)}I^{40} T_{ij}^{E2,40} \right]. \quad (2)$$

The remaining harmonics read

$$T^{E2,20} = \frac{1}{8} \left(\frac{15}{\pi}\right)^{1/2} \sin^2 \theta (\hat{\theta} \otimes \hat{\theta} - \hat{\phi} \otimes \hat{\phi}), \quad (3)$$

$$T^{B2,30} = \frac{1}{8} \left(\frac{105}{\pi} \right)^{1/2} \cos\theta \sin^2\theta (\hat{\theta} \otimes \hat{\phi} + \hat{\phi} \otimes \hat{\theta}), \quad (4)$$

$$T^{E2,40} = \frac{9}{8} \left(\frac{5}{\pi} \right)^{1/2} \sin^2\theta \left(1 - \frac{7}{6} \sin^2\theta \right) (\hat{\theta} \otimes \hat{\theta} - \hat{\phi} \otimes \hat{\phi}). \quad (5)$$

The loss of energy by gravitational radiation, in the case of an infinitely thin axisymmetric disk treated in the first post-Newtonian approximation, takes the form [7]

$$\frac{dE}{dt} = -\frac{G}{32\pi c^5} \langle |^{(3)}I^{20}|^2 \rangle, \quad (6)$$

where angular brackets denote averaging over time. It is easily seen that there is no loss of angular momentum as only the multipole moments with $m = 0$ are nonvanishing. Additionally, the linear momentum stays unchanged and, of course, the baryonic mass of the system is con-

served too.

At the first post-Newtonian approximation only the symmetric and trace-free multipole moments have been related to the matter variables in a mathematically sound manner [9]. In terms of the symmetric and trace-free multipole moments our spherical multipole moments are given by

$$I^{20} = 4 \left(\frac{3\pi}{5} \right)^{1/2} I_{33}, \quad (7)$$

$$S^{30} = -2 \left(\frac{5\pi}{21} \right)^{1/2} J_{333}, \quad (8)$$

$$I^{40} = \frac{1}{18} (5\pi)^{1/2} I_{3333}. \quad (9)$$

For a perfect fluid with vanishing pressure (incoherent matter or dust) the symmetric trace-free multipole moments can be written as (also see, e.g., [4])

$$I_{ij} = \int d^3x \rho \left(1 + \frac{2}{c^2} (v^2 + U) \right) x^{(i} x^{j)} + \frac{1}{14c^2} \frac{d^2}{dt^2} \int d^3x \rho x^2 x^{(i} x^{j)} - \frac{20}{21c^2} \frac{d}{dt} \int d^3x \rho v^k x^{(i} x^j x^{k)}, \quad (10)$$

$$J_{ijk} = \int d^3x \rho x^{(i} x^j \epsilon^{k)ab} x^a v^b, \quad (11)$$

$$I_{ijkl} = \int d^3x \rho x^{(i} x^j x^k x^{l)}, \quad (12)$$

where ρ and v^i denote the proper baryonic mass density and the velocity three-vector field of the dust, respectively. U is the absolute value of the Newtonian gravitational potential. The angular brackets around the indices means taking the symmetric and trace-free part of the enclosed tensor.

III. OSCILLATORY MOTION OF A ROTATING DISK OF DUST

For later reference we briefly summarize the solution of the motion of a dusty disk in the first post-Newtonian approximation. The disk is assumed to be located in the plane $x^3 = 0$ and the metric of three-space is taken in isotropic form. The planar polar coordinates shall be denoted by r and φ .

The surface density Σ and the radial and azimuthal velocities v_r and v_φ , respectively, can be represented as (see paper I)

$$\Sigma(r, t) = \sigma(t) \sqrt{1 - a^2} \left[1 + \frac{1}{2} \kappa(t) a^2 \right], \quad (13)$$

$$v_r(r, t) = -r[f(t) + \lambda(t)a^2], \quad (14)$$

$$v_\varphi(r, t) = r[\Omega(t) + \omega(t)a^2]. \quad (15)$$

Here $a(r, t)$ is defined as r/r_d , where $r_d(t)$ denotes the radius of the disk. Σ is related to ρ through $\rho = \frac{1}{\sqrt{-g_{33}}} \delta(x^3) \Sigma$ (space-time signature -2), where g_{33} is the x^3 -coordinate metric component in isotropic Cartesian space coordinates.

The explicit expressions for the purely time-dependent functions have been obtained in paper I in the case of an oscillating and vibrating disk. Introducing the normalized radial extension of the disk, $X(t) = r_d(t)/R_d$, where R_d denotes the maximal radius of the disk [in the following we choose the origin of time such that $X(0) = 1$], then the functions σ , κ , $\tilde{f} = f + \lambda$, $\tilde{\Omega} = \Omega + \omega$ (rotational angular frequency at the rim of the disk), λ , and ω are given by

$$\sigma(t) = \frac{\sigma_0}{X^2(t)} \left[1 - \frac{27C}{4c^2 R_d} \left(\frac{1}{X(t)} - 1 \right) \right], \quad (16)$$

$$\kappa(t) = \frac{C}{12c^2 R_d} \left[\frac{165}{X(t)} - 128 \left(1 - \frac{\xi_N^2}{2} \right) \right], \quad (17)$$

$$\tilde{f}(t) = -\frac{\dot{X}(t)}{X(t)}, \quad (18)$$

$$\tilde{\Omega}(t) = \frac{\tilde{\Omega}_0}{X^2(t)} \left[1 - \frac{4C}{c^2 R_d} \left(\frac{1}{X(t)} - 1 \right) \right], \quad (19)$$

$$\lambda(t) = -\frac{11C}{8c^2 R_d} \frac{\dot{X}(t)}{X^2(t)}, \quad (20)$$

$$\omega(t) = \frac{3C\tilde{\Omega}_0}{4c^2 R_d X^2(t)} \left(\frac{1}{X(t)} + \frac{13}{32} \frac{1}{\xi_N^2} \right). \quad (21)$$

In the equations above the initial conditions $\sigma_0 = \sigma(0)$, $\tilde{\Omega}_0 = \tilde{\Omega}(0)$, and $R_d = r_d(0)$ can be specified freely. The two constants C and ξ_N^2 are defined as $C = \frac{\pi^2 G \sigma_0 R_d^2}{4}$ and $\xi_N^2 = \frac{\tilde{\Omega}_0^2 R_d^3}{2C}$.

Finally, the solution for $X(t)$, in parametric form with running parameter u , reads

$$X(t) = \frac{1 - e_r \cos u}{1 + e_r}, \quad (22)$$

$$\frac{2\pi}{P}t = u - e_t \sin u - \pi, \quad (23)$$

where

$$\frac{2\pi}{P} = \frac{4}{3\pi GM_0} \left(\frac{-5E}{M_0} \right)^{3/2} \left(1 + \frac{55}{14} \frac{E}{M_0 c^2} \right), \quad (24)$$

$$e_t^2 = 1 + \frac{5E}{M_0} \left(\frac{10L}{3\pi GM_0^2} \right)^2 \left(1 + \frac{65}{7} \frac{E}{M_0 c^2} \right) + \frac{165}{14} \frac{E}{M_0 c^2}, \quad (25)$$

$$e_r^2 = 1 + \frac{5E}{M_0} \left(\frac{10L}{3\pi GM_0^2} \right)^2 \left(1 - \frac{565}{56} \frac{E}{M_0 c^2} \right) - \frac{425}{56} \frac{E}{M_0 c^2}. \quad (26)$$

P is the oscillation period, i.e., the time difference between two consecutive maximal extensions of the disk, as measured far away from the system; the ‘‘eccentricities’’ e_t and e_r serve as two constant parameters.

The radius R_d of the disk is given by

$$R_d = a_r(1 + e_r), \quad (27)$$

$$a_r = -\frac{3\pi GM_0^2}{20E} \left(1 + \frac{437}{112} \frac{E}{M_0 c^2} \right). \quad (28)$$

M_0 , E , and L denote the baryonic mass, the binding energy, and the angular momentum of the system. All three are dynamical constants of motion. We point out again the similarity of our solution for $X(t)$ with the corresponding solution for a binary system [10].

In terms of M_0 , L , which are both constants in the case of radiation damping, and R_d , σ_0 , and $\tilde{\Omega}_0$ are given by

$$\sigma_0 = \frac{3M_0}{2\pi R_d^2} \left[1 - \frac{3\pi GM_0}{480c^2 R_d} (229 + 88\tilde{\xi}_N^2) \right], \quad (29)$$

$$\tilde{\Omega}_0 = \frac{5L}{2M_0 R_d^2} \left[1 - \frac{3\pi GM_0}{140R_d c^2} \left(28 + 21\tilde{\xi}_N^2 - \frac{585}{256} \frac{1}{\tilde{\xi}_N^2} \right) \right], \quad (30)$$

with

$$\tilde{\xi}_N^2 = \frac{25L^2}{3\pi GM_0^3 R_d}. \quad (31)$$

Defining $\xi^2 = 1 - e_r$, in the Newtonian limit $\xi^2 - \xi_N^2$ and $\xi^2 - \tilde{\xi}_N^2$ tend to zero. Obviously, for $e_r = 0$ the oscillations vanish. However, in this limit the disk is not rotating rigidly beyond the Newtonian dynamics. The minimal angular frequency at the center of the disk, Ω_0 , is related to the corresponding angular frequency at the rim of the disk, $\tilde{\Omega}_0$, by

$$\frac{\tilde{\Omega}_0 - \Omega_0}{\Omega_0} = \frac{9\pi GM_0}{32R_d c^2} \left(1 + \frac{13}{32} \frac{1}{\tilde{\xi}_N^2} \right). \quad (32)$$

In the limit of vanishing oscillations, $\tilde{\xi}_N^2 = 1$, this expression is still different from zero (see also paper I).

IV. GRAVITATIONAL RADIATION DAMPING

A. Leading-order damping

Let us start with the leading-order damping, i.e., the Newtonian damping. For this we need to know

$$I_{33} = -\frac{1}{3} \int d^3x r^2 \rho = -\frac{2}{15} M_0 R_d^2 \frac{(1 - e \cos u)^2}{(1 + e)^2}, \quad (33)$$

and readily find (notice $e_t = e_r = e$ in the Newtonian limit)

$$\frac{dE}{dt} = -\frac{64}{3375\pi^2} \frac{c^5}{G} \left(\frac{3\pi GM_0^2}{10Lc} \right)^{10} e^2 (1 - e^2)^{3/2} \times \left(1 + \frac{1}{4} e^2 \right), \quad (34)$$

where the time average has been taken over the period P . The Newtonian energy E can be written as

$$\frac{-5E}{M_0} = \left(\frac{3\pi GM_0^2}{10L} \right)^2 (1 - e^2). \quad (35)$$

Differentiating the last equation with respect to time, taking into account that L and M_0 are constants, and combining with the equation before results in a simple differential equation for $z := e^2$:

$$\frac{dz}{dt} = -\gamma_N z \left(1 + \frac{1}{4} z \right) (1 - z)^{3/2}, \quad (36)$$

where

$$\gamma_N = \frac{64}{675\pi^2} \frac{c^3}{GM_0} \left(\frac{3\pi GM_0^2}{10Lc} \right)^8. \quad (37)$$

For two initial values of z the time derivative of z vanishes, $z = 0$ and $z = 1$. In the first case there are no oscillations, and in the second case there is purely radial collapse. Obviously, for z unequal to zero or one, z is monotonically decreasing, approaching zero exponentially as $e^{-\gamma_N t}$; i.e., γ_N is the asymptotic damping constant.

The changes in time of the period P and the radius R_d are most easily obtained, knowing the solution for e^2 , by use of the relations

$$\frac{2\pi}{P} = \frac{4}{3\pi GM_0} \left(\frac{3\pi GM_0^2}{10L} \right)^3 (1 - e^2)^{3/2} \quad (38)$$

and

$$\frac{3\pi GM_0}{4R_d} = \left(\frac{3\pi GM_0^2}{10L} \right)^2 (1 - e). \quad (39)$$

B. Higher-order damping

For the post-Newtonian radiation damping we need to evaluate

$$I_{33} = -\frac{1}{3} \int d^3x r^2 \varrho \left(1 + \frac{2}{c^2} (v^2 + U) \right) - \frac{1}{42c^2} \frac{d^2}{dt^2} \int d^3x r^4 \varrho + \frac{4}{21c^2} \frac{d}{dt} \int d^3x r^3 \varrho v_r.$$

A straightforward calculation yields

$$I_{33} = -\frac{2}{15} M_0 R_d^2 \frac{(1 - e_r \cos u)^2}{(1 + e_r)^2} - \frac{L^2}{M_0 c^2} \frac{819 - 640e_r^2 + 1157e_r \cos u - 1336e_r^2 \cos^2 u}{2352(1 - e_r^2)}. \quad (40)$$

The post-Newtonian energy loss is obtained after a longer calculation from Eq. (6) in the form

$$\frac{dE}{dt} = -\frac{64}{3375\pi^2} \frac{c^5 \alpha^{10}}{G} e_r^2 (1 - e_r^2)^{3/2} \left[1 + \frac{1}{4} e_r^2 - \alpha^2 \frac{4283 + 4069e_r^2 - \frac{841}{8} e_r^4}{392} \right], \quad (41)$$

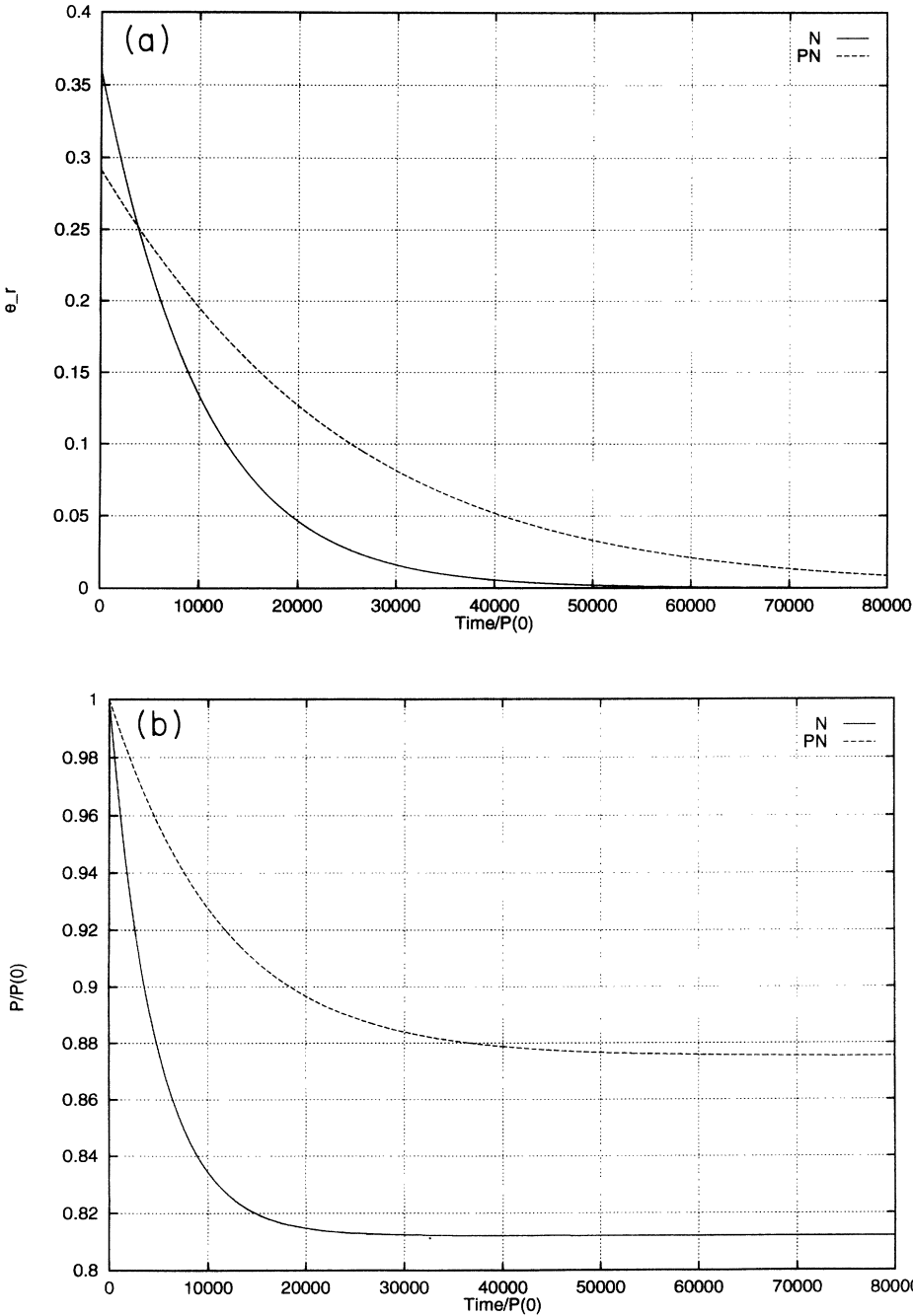


FIG. 1. The long-term time evolution of parameters of an oscillating disk, damped by gravitational radiation emission. Plotted are the variation of the eccentricity e_r (a), the period P (b), and the total energy (c), where the solid lines refer to the lowest-order (Newtonian) and the dashed lines to the first post-Newtonian approximations.

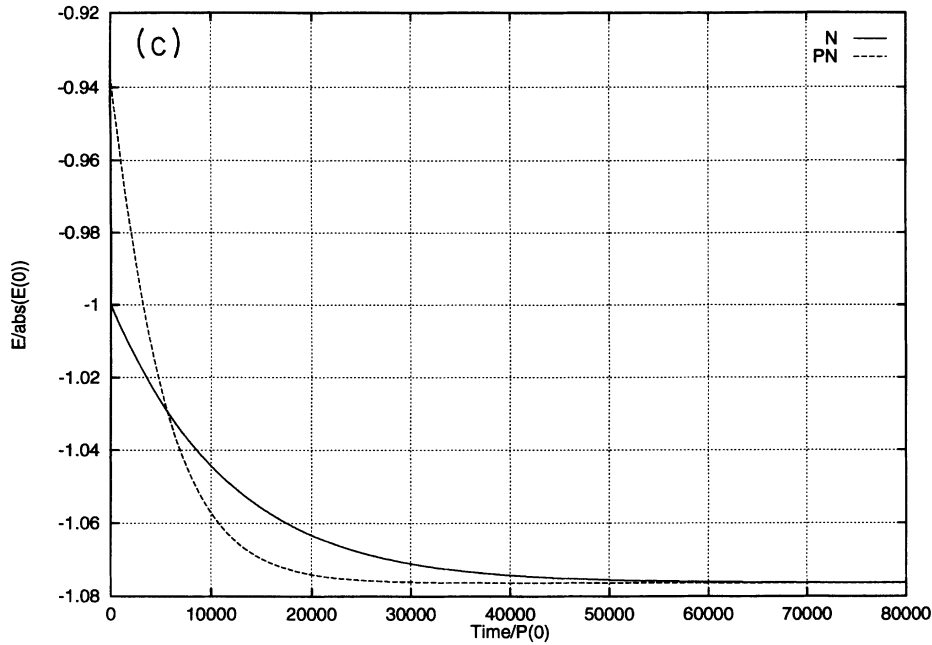


FIG. 1. (Continued).

where

$$\alpha = \frac{3\pi GM_0^2}{10Lc}. \quad (42)$$

Differentiation of Eq. (26) with respect to time and taking into account the energy loss (41) yields the following equation for $z := e_r^2$:

$$\frac{dz}{dt} = -\gamma z(1-z)^{3/2} \left[1 + \left(1 - \frac{18321}{392} \alpha^2 \right) \frac{z}{4} - \frac{2323}{49} \frac{\alpha^2 z^2}{64} \right], \quad (43)$$

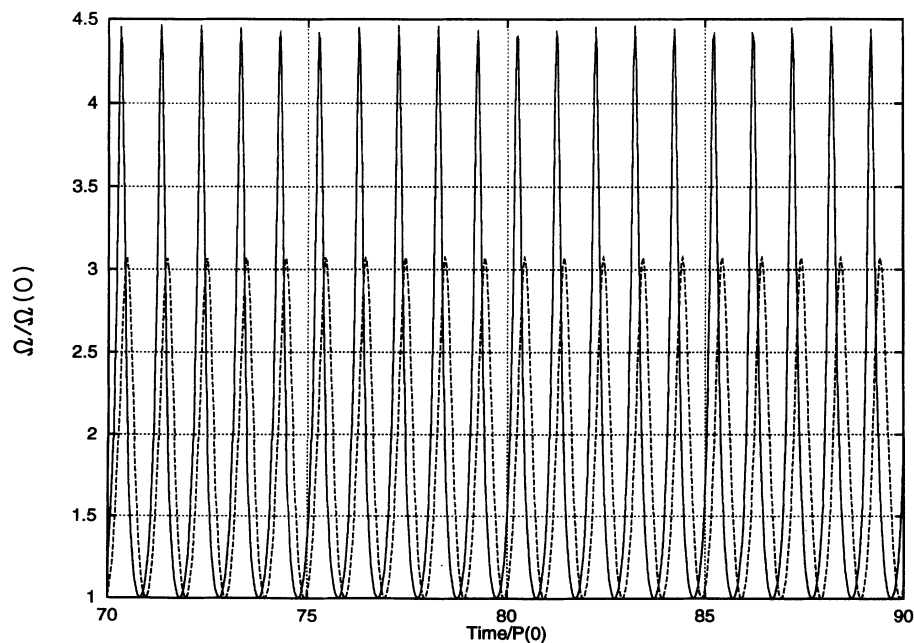


FIG. 2. The damping-induced variations of the orbital angular frequency at the disk's outer rim $\tilde{\Omega}$, normalized to the initial value, versus time for the first-order (solid line) and higher-order (dashed line) approximations. The offset in the time coordinate has been introduced to show the accumulated phase shift of the Newtonian and post-Newtonian cases.

where

$$\gamma = \gamma_N \left(1 - \frac{412}{49} \alpha^2 \right), \quad (44)$$

with, as above,

$$\gamma_N = \frac{64}{675\pi^2} \frac{c^3 \alpha^8}{GM_0}. \quad (45)$$

Apparently the higher-order correction reduces the asymptotic damping constant. The changes in time of all the other quantities are easily obtained from the time variation of z . The appropriate representation of, e.g., the energy, reads

$$\frac{-5E}{M_0 c^2} = \alpha^2 (1-z) \left[1 - \frac{1}{56} (28 - 113z) \alpha^2 \right]. \quad (46)$$

A useful quantity is $P\gamma$, the oscillation period divided by the damping time, which gives a measure of how much damping occurs per oscillation period. As function of z it reads

$$P\gamma = \frac{32}{225} \alpha^5 (1-z)^{-3/2} \left[1 - \frac{1}{784} (5388 + 2989z) \alpha^2 \right]. \quad (47)$$

To demonstrate the long-term evolution of the physical parameters we consider a model system consisting of a cold gaseous disk after a merging process of two massive white dwarfs. Let us assume that the formed disk has a total baryonic mass of $2.5 M_\odot$ spread within a radius of 200 km. This size of the disk is somewhat smaller than the initial white dwarf radii and may represent a disk formed by a merger but which has already evolved further. Since in a merging process the baryonic mass, the angular momentum, and energy of the system remain approximately unchanged, the formed disk will oscillate around an equilibrium state [nonoscillation would need $e_r = e_t = 0$, implying a particular relation between M_0 , L , and E ; see Eqs. (25) and (26)]. For the initial amplitude we assume a value of 0.5 for the ratio of the minimum to the maximum extension of the disk, which corresponds to $\xi = 0.8$. This situation makes the disk just weakly relativistic and the present analysis is ideally suited.

To illustrate the effects, we integrated Eqs. (36) and (43) numerically, taking the same values for M_0 , L , and as well for $P(0)$. In Fig. 1 the obtained time variations of the e_r , P , and E are plotted. In each case we compare the leading-order term, labeled by N , and the higher-order term, labeled by PN . The time axis is scaled with respect to the initial period of the disk, which is about 1.3×10^{-2} sec. According to Eq. (46), the energies go asymptotically to the same value since the eccentricity

approaches zero [Fig. 1(a)]. The post-Newtonian damping occurs on longer time scales. We are aware, however, that in realistic cases viscous damping is very likely to dominate the gravitational damping.

The Newtonian and post-Newtonian periods begin to diverge initially and are approaching different values, where the final post-Newtonian value is higher than its Newtonian counterpart; see Eq. (24). The energies [Fig. 1(c)] are approaching identical values [see Eq. (46)]. The different periods lead to a phase shift of the oscillations. This is demonstrated in Fig. 2, where the angular velocity is plotted versus time with an offset of 70 to show the accumulated phase shift more clearly. The observant reader may notice that the amplitude differences of Newtonian and post-Newtonian motions are seemingly in disagreement with paper I (Fig. 1). Note, however, that in the present work we plot the curves corresponding to identical baryonic mass, while in paper I the gravitational mass was identical.

V. GRAVITATIONAL WAVEFORMS

A. Leading-order waveform

The gravitational wave in leading order is determined by the Newtonian expression for ${}^{(2)}I^{20}$. In explicit terms, as function of time t , it reads

$${}^{(2)}I^{20} = -16 \left(\frac{\pi}{15} \right)^{1/2} E \left(1 - \frac{1}{1 - e \cos u} \right), \quad (48)$$

with

$$u - e \sin u = \frac{2\pi}{P} t + \pi. \quad (49)$$

It seems worthwhile to point out the strong difference on the time dependence of ${}^{(2)}I^{20}$ in comparison to the corresponding expression in the scalar gravity theory as discussed in [11].

B. Higher-order waveform

In addition to I_{33} of Eq. (40) the following radiative multipole moments have to be evaluated additionally to get the higher-order waveform:

$$J_{333} = -\frac{1}{5} \int d^3 x r^3 \varrho v_\varphi,$$

$$I_{3333} = \frac{3}{35} \int d^3 x r^4 \varrho.$$

After differentiation with respect to time and use of Eqs. (7)–(9) we find for the spherical components of the higher-order waveform the expressions

$${}^{(2)}I^{20} = -\frac{16}{15} \sqrt{15\pi} E \left(1 - \frac{1}{1 - e_r \cos u} \right) + \frac{\sqrt{15\pi} E^2}{147 M_0 c^2} \left(48 - \frac{1567}{1 - e_r \cos u} + \frac{303}{(1 - e_r \cos u)^2} + \frac{1216(1 - e_r^2)}{(1 - e_r \cos u)^3} \right), \quad (50)$$

$${}^{(3)}S^{30} = -\frac{(40)^2}{(21)^2} \sqrt{\frac{21}{\pi}} \frac{L}{GM_0} \left(\frac{-E}{M_0} \right)^{5/2} \frac{e_r \sin u}{(1 - e_r \cos u)^3}, \quad (51)$$

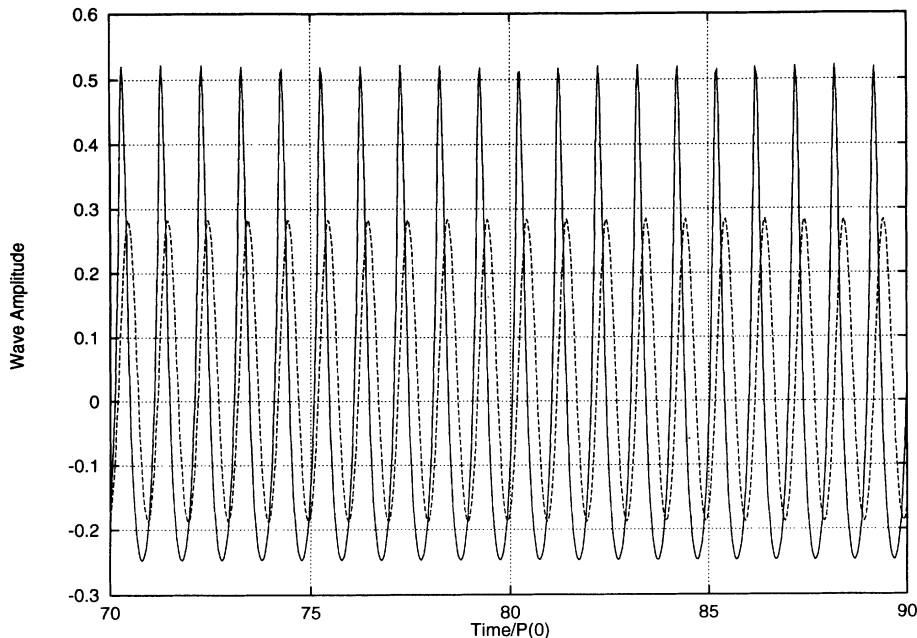


FIG. 3. The asymptotic quadrupole waveform ${}^{(2)}I^{20}$ in units of $(16/15)(15\pi)^{1/2}E(0)$ versus time for the radiation damped oscillating disk as described in Sec. IV B. Plotted is the the first-order (solid line) and higher-order (dashed line) approximations. The offset in the time coordinate has been introduced to show the accumulated phase shift of the Newtonian and post-Newtonian cases.

$${}^{(4)}I^{40} = \frac{48\sqrt{5\pi}E^2}{(21)^2M_0} \left[6 - \frac{6}{1 - e_r \cos u} - \frac{5}{(1 - e_r \cos u)^2} + \frac{5(1 - e_r^2)}{(1 - e_r \cos u)^3} \right]. \quad (52)$$

The parameter u is now given by

$$u - \left(1 + \frac{155}{16} \frac{E}{M_0 c^2} \right) e_r \sin u = \frac{2\pi}{P} t + \pi. \quad (53)$$

The changes in time of eccentricity and period lead to phase shifts of the Newtonian waveform (48) and the post-Newtonian waveform (50). This is demonstrated in Fig. 3, where the two asymptotic wave amplitudes ${}^{(2)}I^{20}$ of our model system as described above are plotted, normalized to $\frac{16}{15}\sqrt{15\pi}E(0)$. The first-order waveform (48) is very similar to the one presented in [2, Fig. 1]; the deviation in amplitudes stems from the different parameter ξ used. The higher-order waveform has a reduced amplitude and a phase shift. The contributions of the current-octupole moment S^{30} and mass-hexadecapole moment I^{40} are at least one order of magnitude smaller than the post-Newtonian contribution to the mass-quadrupole moment I^{20} . Thus, we will not discuss them any further.

VI. CONCLUSIONS

The gravitational-wave emission and radiation damping of an oscillating and rotating post-Newtonian disk of dust have been treated in this paper in full analytical detail. Several plots have made transparent important relations.

The main result of the paper can be seen in exploiting the relation between the Newtonian and post-Newtonian damping and emission. In [2] the wave emission has been calculated for a counterrotating disk with vanishing net

angular momentum. We have shown that on small time scales the changes of the relative phase relations of the oscillating quantities, orbital angular frequency of the rim of the disk, and gravitational-wave amplitude are of importance, whereas on longer time scales also the changes of the relations of their amplitudes become important.

In the following let us discuss a possible application of our model: oscillating disks with a few hundred km radius, which may result after the merging of binary white dwarf systems with a total of 2.5 solar masses. The oscillation periods are around 0.013 sec (corresponding to a 76.9 Hz frequency), and the gravitational-wave amplitudes h reach 1.5×10^{-21} for such a disk located at a distance of about 1 Mpc (extension of the Local Group). Note that because of axisymmetry the gravitational-wave frequency is identical to the inverse of the oscillation period $1/P$ of the disk. Those waves fit nicely into the gravitational-wave detection program on Earth [1]. However, shortly after the merging process of white dwarf binaries, oscillating disks may occur with periods in the regime of several seconds. The corresponding gravitational waves are good candidates for detection by space borne detectors [1]. The frequency of white dwarf mergers within the Local Group can be estimated to be 1 per 5 years [12] and [13]. The application to white dwarf binaries after coalescence is not the only application of importance. One may consider also the coalescence of neutron star binaries or compact supermassive disks of about 10^6 solar masses located at the center of active galactic nuclei. The related physical quantities, e.g., the gravitational-wave amplitude, can easily be obtained from the merging white dwarf example by rescaling mass and extension.

- [1] K. S. Thorne, in *300 Years of Gravitation*, edited by S. W. Hawking and W. Israel (Cambridge University Press, Cambridge, England, 1987).
- [2] A. M. Abrahams, S. L. Shapiro, and S. A. Teukolsky, (unpublished).
- [3] W. Kley and G. Schäfer, preceding paper, *Phys. Rev. D* **50**, 6217 (1994), referred to as paper I.
- [4] L. Blanchet, T. Damour, and G. Schäfer, *Mon. Not. R. Astron. Soc.* **242**, 289 (1990).
- [5] L. Blanchet and G. Schäfer, *Mon. Not. R. Astron. Soc.* **239**, 845 (1989).
- [6] W. Junker and G. Schäfer, *Mon. Not. R. Astron. Soc.* **254**, 146 (1992).
- [7] K. S. Thorne, *Rev. Mod. Phys.* **52**, 299 (1980).
- [8] R. Mönchmeyer, G. Schäfer, E. Müller, and R. E. Kates, *Astron. Astrophys.* **246**, 417 (1991).
- [9] L. Blanchet and T. Damour, *Ann. Inst. Henri Poincaré* **50**, 377 (1989).
- [10] T. Damour and N. Deruelle, *Ann. Inst. Henri Poincaré* **43**, 107 (1985).
- [11] S. L. Shapiro and S. A. Teukolsky, *Phys. Rev. D* **49**, 1886 (1994).
- [12] D. Hils, P. L. Bender, and R. F. Webbink, *Astrophys. J.* **360**, 75 (1990).
- [13] M. Livio, in *Theory of Accretion Disks*, edited by F. Meyer, W. J. Duschl, J. Frank, and E. Meyer-Hofmeister (Kluwer Academic Publishers, Dordrecht, 1989).